

Spin-dynamic field coupling in strongly THz driven semiconductors : local inversion symmetry breaking

Kristinn Johnsen

NORDITA, Blegdamsvej 17, DK-2100 Copenhagen Ø, Denmark

(October 24, 2018)

We study theoretically the optics in undoped direct gap semiconductors which are strongly driven in the THz regime. We calculate the optical sideband generation due to nonlinear mixing of the THz field and the near infrared probe. Starting with an inversion symmetric microscopic Hamiltonian we include the THz field nonperturbatively using non-equilibrium Green function techniques. We find that a self induced relativistic spin-THz field coupling locally breaks the inversion symmetry, resulting in the formation of odd sidebands which otherwise are absent.

I. INTRODUCTION

Optical properties of semiconductors are sensitive to external conditions such as strong static electric fields being applied to the sample. This was predicted more than 40 years ago by Franz and Keldysh [1] and leads to the Franz-Keldysh effect. The effect manifests itself in finite absorption within the gap, near the band edge, and modulation of the above gap absorption spectrum. The effect can be understood in terms of tunneling assisted absorption. This work was generalized to oscillating external fields, $\vec{E}(t) = \vec{E} \cos(\Omega t)$, by Yacoby [2] 30 years ago. Yacoby concluded that similar effects to the Franz-Keldysh effect manifest provided that the ponderomotive energy,

$$E_f = \hbar\omega_f = \frac{e^2 E^2}{4m_r \Omega^2}, \quad (1)$$

magnitude is similar to the photon energy, $\hbar\Omega$, of the external field, i.e.

$$\gamma = \frac{\omega_f}{\Omega} = \frac{e^2 E^2}{4\hbar m_r \Omega^3} \sim 1. \quad (2)$$

Here $1/m_r = 1/m_c + 1/m_v$ is the reduced mass of the effective valence and conduction band masses m_v and m_c respectively. Then the field induced effects extend a few $\hbar\Omega$ around gap and may be viewed as being due to a combination of quantum mechanical tunneling and multi photon processes. Experimentally it is exceedingly difficult to fulfill the condition (2) such that the effect extends over a range which can be resolved experimentally. The advent of the free electron laser as a source of intense coherent radiation in the THz regime [3] has made it possible to enter the regime $\gamma \sim 1$, which now has come to be known as the dynamical Franz-Keldysh (DFK) regime. Works reporting on optical experiments in the DFK regime include Refs. [4–8]. This has also led to renewed theoretical interest of THz electro optics, see e.g. Refs. [9–13]. It has been shown that the physical signature of the DFK effect is enhanced with reduced dimensionality [10], which has led to experimental investigation of the two dimensional analogue of Yacoby's prediction in quantum wells at low temperatures [4]. Of particular relevance to the present work is the observation of optical sidebands in the transmission spectrum at frequencies $\omega_p \pm 2n\Omega$, where ω_p is the probe frequency and n is an integer. Thus the sidebands only appear at even multiples of the driving frequency Ω in quantum wells. This observation can be understood as being a direct consequence of the underlying inversion symmetry of the system [14], e.g. the dispersion has the property $\epsilon_n(\vec{k}) = \epsilon_n(-\vec{k})$, n is the band index. We remark from the onset that it is assumed that the THz field does not induce interband coupling [15]. Absence of odd sidebands has also been observed in the presence of strong quantizing magnetic fields [6]. In Ref. [8] it has now been experimentally demonstrated that odd sidebands appear if the inversion symmetry is broken by driving the system such that the field oscillates in the growth direction of an asymmetric quantum well. These observations support the assumption that the THz field only induces intraband dynamics. In the light of these observations and the theoretical understanding thereof it therefore comes as a curious surprise that odd sideband formation is observed of resonance, e.g. away from the gap, in apparently inversion symmetric bulk samples [16]. In the present work we theoretically demonstrate that inversion symmetry breaking results from spin-dynamic field coupling leading to the formation of odd sidebands. We refer to the well known relativistic effect that a charged particle traveling with velocity \vec{v} in an electric field \vec{E} experiences

an effective magnetic field proportional to $\vec{v} \times \vec{E}$ which couples to the particles spin degree of freedom via a Zeeman term, see e.g. Ref. [[19]]. In the present case the electric field is the strong THz field driving the system.

The article is organized as follows; in Sec. II we define the theoretical model and calculate the sideband intensities neglecting the spin-THz field coupling and show how only even sidebands appear, in Sec. II we calculate effect of the spin-THz field coupling and finally in Sec. IV we discuss the physical consequences of our results and present numerical calculations for sideband generation in GaAs and InAs.

II. THE MODEL

In this section we define the model which we shall study. Our approach is to apply non-equilibrium Green function techniques to include the THz field nonperturbatively. This can be done analytically and the resulting Green functions form the starting point for our subsequent calculations, which is to account for the relativistic term perturbatively in the Born approximation. The resulting Green functions are then applied to determine the interband susceptibility which describes the linear response of the system to a weak optical near infrared probe field.

We consider a direct gap undoped bulk semiconductor subject to an intense linearly polarized THz field, $E_{THz}(t)$. We shall assume that effects due to the finite wave-vector are negligible, that is we assume that the THz field is uniform. Thus the system considered remains translationally invariant and the wave vector is still a good quantum number. We shall model the system with a four band model which is a generalization of the model introduced in Ref. [[15]]. A conduction band and a valence band, each carrying one of two spin states. We start our analysis with the second quantized Hamiltonian

$$H^0 = \sum_{\alpha=\{c,v\},\sigma,\vec{k}} \epsilon_{\alpha\sigma} [\hbar\vec{k} + e\vec{A}(t)] c_{\alpha\sigma\vec{k}}^\dagger c_{\alpha\sigma\vec{k}}. \quad (3)$$

Here σ is the spin state index, α the band index and k is the wave vector of the state. The THz field is introduced nonperturbatively via the vector potential $\vec{A} = -\vec{E} \sin(\Omega t)/\Omega$. We shall assume that the THz field is oriented in the \hat{z} -direction. The probe has wave vector \vec{q} and is oriented such that it forms an angle θ to the \hat{z} -direction, see Fig. 1. For simplicity, we shall assume that the bands are parabolic, even away from the gap. We assume that

$$\epsilon_{c\sigma}(\vec{p}) = \frac{p^2}{2m_c} + \epsilon_g \quad (4)$$

for the conduction band. Here m_c is effective mass for the conduction band and ϵ_g is energy gap of the semiconductor. For the valence band we describe the dispersion as

$$\epsilon_{v\sigma}(\vec{p}) = -\frac{p^2}{2m_v}, \quad (5)$$

where the m_v is the effective mass of valence band electrons. Note that $\epsilon_{\alpha\sigma}(\vec{p}) = \epsilon_{\alpha\sigma}(-\vec{p})$, so the initial Hamiltonian is inversion symmetric. Furthermore, we shall assume that the interband dipole matrix elements $d_{cv\sigma_c\sigma_v}$ are locally independent of the wave vector, but that they depend on the general underlying symmetries of the Brillouin zone being probed. For instance, near a point of high symmetry like the Γ -point we take $d_{cv\sigma_c\sigma_v} \propto \delta_{\sigma_c\sigma_v}$, reflecting the near gap selection rules. Away from the Γ -point these selection rules are not in force, and we shall assume that all the matrix elements are finite but constant. Below we shall thus consider two distinct regimes, the *near gap regime* characterized by the selection rules and the *far regime*, where the selection rules are not in force.

The relevant quantity to study in order to glean the optical properties of the system, is the interband susceptibility. The non-equilibrium causal interband susceptibility on the Keldysh contour is given by [14]

$$\chi_{cv\beta\vec{q},t,t'} = -\frac{i}{\hbar} \int \frac{dk}{(2\pi)^3} g_{c\sigma_c\sigma'_c}(\vec{k} + \vec{q}, t, t') g_{v\sigma'_v\sigma_v}(\vec{k}, t', t), \quad (6)$$

where $\beta = (\sigma_c\sigma_v\sigma'_c\sigma'_v)$ and the contour ordered Keldysh Green functions are defined by

$$g_{\alpha\sigma\sigma'}(\vec{k}, t, t') = -i \langle T_c [c_{\alpha\sigma\vec{k}}(t) c_{\alpha'\sigma'\vec{k}}^\dagger(t')] \rangle. \quad (7)$$

For an overview on non-equilibrium Green functions see [17]. The physically relevant susceptibility is the real time retarded susceptibility. We analytically continue the causal susceptibility using the Langreth rules [18] and find that

$$\chi_{cv\beta}^r(\vec{q}, t, t') = -\frac{i}{\hbar} \int \frac{dk}{(2\pi)^3} \left[g_{c\sigma_c\sigma'_c}^<(\vec{k} + \vec{q}, t, t') g_{v\sigma'_v\sigma_v}^a(\vec{k}, t', t) + g_{c\sigma_c\sigma'_c}^r(\vec{k} + \vec{q}, t, t') g_{v\sigma'_v\sigma_v}^<(\vec{k}, t', t) \right]. \quad (8)$$

In the quasiparticle picture one describes the lesser function, $g^<$, as a distribution function f times the spectral function via $g^< = ifa$. The spectral function is given by $a = i(g^r - g^a)$ in a non-equilibrium system. In equilibrium this generalization becomes the familiar $a_{eq} = 2\text{Im}g^r$.

In an undoped semiconductor all the valence band is occupied, hence the distribution function is one, but no states in the conduction band are occupied and the corresponding distribution function is zero. We thus put $g_v^< = -(g_v^r - g_v^a)$ and $g_c^< = 0$. The interband susceptibility becomes

$$\chi_{cv\beta}^r(\vec{q}, t, t') = -\frac{i}{\hbar} \int \frac{dk}{(2\pi)^3} g_{c\sigma_c\sigma'_c}^r(\vec{k} + \vec{q}, t, t') g_{v\sigma'_v\sigma_v}^a(\vec{k}, t', t). \quad (9)$$

Probing the system with a weak beam $E_p(\vec{q}, \omega_p t) \sim E_p e^{-i\omega_p t}$, the linearly induced interband polarization is

$$P_{cv}(t) = e^2 E_p \sum_{\sigma'_c\sigma'_v\sigma_c\sigma_v} d_{cv\sigma_c\sigma_v} d_{cv\sigma'_c\sigma'_v} \int dt' \chi_{cv\sigma_c\sigma_v\sigma'_c\sigma'_v}^r(\vec{q}, t, t') e^{-i\omega_p t'}. \quad (10)$$

Driving the system with THz frequency Ω the induced polarization will be of the form

$$P_{cv}(t) = e^2 E_p \sum_n \eta_n(\omega_p) e^{-i(\omega_p + n\Omega)t}, \quad (11)$$

which spectrally is a comb of oscillating dipoles giving rise to sidebands irradiating with intensity proportional to $I_n(\omega_p) = |\eta_n(\omega_p)|^2$ and frequency $\omega_p + n\Omega$. The absorption of the probe is proportional to $\text{Im}\eta_0(\omega_p)$.

Neglecting relativistic effects, the Green functions obeys the Dyson equation

$$\{i\hbar\partial_t - \epsilon_{\alpha\sigma}(\hbar\vec{k} + e\vec{A}(t))\} g_{\alpha\sigma\sigma'}^{0r/a}(\vec{k}, t, t') = \hbar\delta_{\sigma\sigma'}\delta(t - t'), \quad (12)$$

with the appropriate boundary conditions. These Green functions which include the THz field to all orders form the starting point of our subsequent calculations. Thus our unperturbed Green functions take the THz field into account from the onset. The equations are readily integrated with the results

$$g_{\alpha\sigma\sigma'}^{0r/a}(\vec{k}, t, t') = \pm\hbar\delta_{\sigma\sigma'}\theta(\pm t \mp t') \exp\left\{-i\int_{t'}^t \frac{ds}{\hbar} \epsilon_{\alpha\sigma}(\hbar\vec{k} + e\vec{A}(s))\right\}. \quad (13)$$

Using these Green functions in order to evaluate the interband susceptibility leads to a Gaussian integral in \vec{k} -space which we evaluate with the result

$$\chi_{cv\beta}^{0r}(\vec{q}, \tau, T) = \frac{e^{i\pi/4}}{(2\pi)^{3/2}} \frac{(m_r\Omega)^{3/2}}{\sqrt{\hbar}} e^{-i(\hbar q^2/(2M) + \omega_f + \omega_g)\tau} \sum_n e^{-in\pi/2} f_n^0(\Omega\tau) e^{-i2n\Omega T}. \quad (14)$$

Here $\tau = t - t'$, $T = (t + t')/2$, $M = m_v + m_c$, and we have defined

$$f_n^l(x) = \frac{\theta(x)}{x^{3/2}} \sin^l(x/2) \exp\left(4i\gamma \frac{\sin^2(x/2)}{x}\right) J_n\left(\gamma\left(\sin x - 4\frac{\sin^2(x/2)}{x}\right)\right). \quad (15)$$

Other components of the susceptibility are zero. We thus obtain that

$$\eta_{2n}(\omega_p) = 2d_{cv\uparrow\uparrow} d_{cv\uparrow\uparrow} \frac{e^{i(1-2n)\pi/4}}{(2\pi)^{3/2}} \frac{(m_r\Omega)^{3/2}}{\sqrt{\hbar}} \int_0^\infty d\tau f_n^0(\Omega\tau) e^{i\omega_{qn}\tau}, \quad (16)$$

where we have used that $d_{cv\uparrow\uparrow} = d_{cv\downarrow\downarrow}$ and we have defined $\omega_{qn} = \omega_p + n\Omega - \hbar q^2/(2M) - \omega_f - \omega_g$. The remaining integral is readily evaluated numerically.

A. PHYSICAL IMPLICATIONS

Here several physical results emerge. Sidebands do only appear at frequencies $\omega_p \pm 2n\Omega$, no sidebands involving an odd number of THz photons appear. This is a direct consequence of the inversion symmetry of the Hamiltonian. The response is independent on the relative orientation of the probe and the THz field, which is reflected by that the result only depends on the magnitude of q . In Fig. 2 we illustrate the sideband intensities for the first 4 sidebands as a function of the probe frequency. These results are valid in the near zone, and are in qualitative agreement with the experimental findings reported in [4] for quantum wells. Both the probe and the irradiating sidebands are close to real states, hence the asymmetry around ω_g . The relation $I_n(\omega) = I_{-n}(\omega + n\Omega)$ holds. The probe or the sideband is near the main spectral feature, the band edge in the present case. In the quantum well the main feature is the 1s exciton resonance [7].

III. THE RELATIVISTIC SPIN-THZ FIELD COUPLING

In this section we shall take into account the relativistic effects. The coupling to the spins comes physically about because a moving electron in the presence of an electric field experiences a local magnetic field, proportional to $\vec{v} \times \vec{E}$, which couples to its spin via a Zeeman interaction, see e.g. [19]. This is the effect which gives rise to spin orbit coupling in atoms and solids. In the situation considered here the strong THz field provides the electric field giving rise to the effect. We describe the contribution to the Hamiltonian as

$$U_i(\vec{k}, t) = \alpha_i e \vec{\sigma} \cdot (\vec{k} \times \vec{E}(t)), \quad (17)$$

here α_i , $i = \{c, v\}$, is an effective coupling constant which depends on the material, $\vec{\sigma}$ is a vector of the Pauli matrices and $\vec{E}(t)$ is the intense THz field. With \vec{E} oriented in the \hat{z} direction (17) becomes

$$U_i(\vec{k}, t) = \alpha_i e \begin{pmatrix} 0 & k_y + ik_x \\ k_y - ik_x & 0 \end{pmatrix} E_z(t). \quad (18)$$

Physically the same kind of term has been studied by Raman spectroscopy in asymmetric GaAs quantum wells [20]. Then the external field is static and comes about due to the asymmetry of the quantum well confining potential. The term breaks time reversal symmetry and thus influences weak localization leading to weak anti-localization [21,22]. The important thing for the present study is that α_c has been determined both experimentally [20] and theoretically [21] for GaAs leading to $\alpha_c \approx 5\text{\AA}^2$, and for InAs $\alpha_c \approx 110\text{\AA}^2$. From the point of view of an effective mass picture we estimate the coefficient for the valence band by $\alpha_v = \alpha_c(m_c/m_v)^2$. These parameters are such that they lead to small corrections compared to the remainder of the Hamiltonian. We thus calculate the correction to the Green functions to lowest order in the Born approximation, with the result

$$g_i^{r/a}(\vec{k}, t, t') = g_i^{0r/a}(\vec{k}, t, t') + \int_{-\infty}^{\infty} \frac{ds}{\hbar^2} g_i^{0r/a}(\vec{k}, t, s) U_i(\vec{k}, s) g_i^{0r/a}(\vec{k}, s, t') \quad (19)$$

$$= \begin{pmatrix} 1 & \pm l_i(t, t')(k_y + ik_x) \\ \pm l_i(t, t')(k_y - ik_x) & 1 \end{pmatrix} g_i^{0r/a}(\vec{k}, t, t'), \quad (20)$$

where we have introduced the quantity

$$l_i(t, t') = 2 \frac{\alpha_i e E_z}{\hbar \Omega} \cos\left(\Omega \frac{t+t'}{2}\right) \sin(\Omega(t-t')). \quad (21)$$

Note that $l_i(t, t') = -l_i(t', t)$. Again in this case it is straightforward to perform the \vec{k} integration in order to obtain the interband susceptibility via Eq. (9). The integrals involved are Gaussian times polynomials in \vec{k} . We remark that higher order contributions preserve this structure as well and are thus readily determined. Now the relative orientation of the probe with respect to the driving field becomes important. We assume that \vec{q} is perpendicular to the \hat{x} direction. We find that $\chi_{cv\beta}(\vec{q}, \tau, T) = \chi_{cv\beta}^{0r}(\vec{q}, \tau, T)$ for $\beta \in \{\uparrow\uparrow\uparrow\uparrow, \uparrow\downarrow\uparrow\downarrow, \downarrow\uparrow\downarrow\uparrow, \downarrow\downarrow\downarrow\downarrow\}$,

$$\begin{aligned} \chi_{cv\beta}(\vec{q}, \tau, T) &= \frac{1}{(2\pi)^{3/2}} \frac{2e\alpha_v q_y E_z}{\hbar \Omega} \frac{e^{-i\pi 5/4}}{\sqrt{\hbar}} \frac{m_r^{5/2} \Omega^{3/2}}{m_c} e^{-i(\hbar q^2/(2M) + \omega_f + \omega_g)\tau} \\ &\times \cos(\Omega T) \sum_n e^{-in\pi/2} f_n^1(\Omega\tau) e^{-i2n\Omega T}, \end{aligned} \quad (22)$$

for $\beta \in \{\downarrow\downarrow\downarrow\uparrow, \uparrow\downarrow\uparrow\uparrow, \uparrow\uparrow\downarrow\downarrow, \downarrow\uparrow\downarrow\downarrow\}$,

$$\chi_{cv\beta}(\vec{q}, \tau, T) = \frac{1}{(2\pi)^{3/2}} \frac{2e\alpha_c q_y E_z}{\hbar\Omega} \frac{e^{-i\pi 5/4}}{\sqrt{\hbar}} \frac{m_r^{5/2} \Omega^{3/2}}{m_c} \left(1 - i \frac{m_r}{m_c}\right) e^{-i(\hbar q^2/(2M) + \omega_f + \omega_g)\tau} \times \cos(\Omega T) \sum_n e^{-in\pi/2} f_n^1(\Omega\tau) e^{-i2n\Omega T}, \quad (23)$$

for $\beta \in \{\downarrow\uparrow\uparrow\uparrow, \downarrow\downarrow\uparrow\downarrow, \uparrow\downarrow\uparrow\downarrow, \uparrow\downarrow\downarrow\downarrow\}$. Other components are of second order in α and are negligible. We can now find the sideband intensities from

$$\eta_{2n}(\omega_p) = 2(d_{cv\uparrow\uparrow}d_{cv\uparrow\uparrow} + d_{cv\uparrow\downarrow}d_{cv\uparrow\downarrow}) \frac{e^{i\pi(1-2n)/4}}{(2\pi)^{3/2}} \frac{(m_r\Omega)^{3/2}}{\sqrt{\hbar}} \int_0^\infty d\tau f_n^0(\Omega\tau) e^{i\omega_{qn}\tau} \quad (24)$$

and

$$\eta_{2n+1}(\omega_p) = 4d_{cv\uparrow\uparrow}d_{cv\uparrow\downarrow} \frac{e^{-i\pi(5+2n)/4}}{(2\pi)^{3/2}} \frac{(m_r\Omega)^{3/2}}{\sqrt{\hbar}} \frac{m_r}{m_c} \frac{2e(\alpha_v + \alpha_c(1 - i\frac{m_r}{m_c}))q_y E_z}{\hbar\Omega} \int_0^\infty d\tau (f_n^1(\Omega\tau) - i f_{n+1}^1(\Omega\tau)) e^{i\omega_{qn}\tau} \quad (25)$$

This is the main result of the present work.

IV. RESULTS AND DISCUSSIONS

When $d_{cv\uparrow\downarrow} \ll d_{cv\uparrow\uparrow}$, as is the case near the Γ -point, near resonance, the relativistic effects are suppressed and we obtain the results of the previous section. The relativistic effects, i.e. contributions to the sideband intensity proportional to α_i , manifest themselves in the far zone, away from resonance. The relativistic term leads to the formation of odd sidebands. Thus the inversion symmetry has been broken and relativistic self induced local symmetry breaking has taken place. The inversion symmetry breaking is local because it is only detectable with finite probe wave vector \vec{q} . We say that the symmetry breaking is global if it leads to odd sidebands even when $q \rightarrow 0$. An example of a global symmetry breaking is for instance when a linear term is present in the dispersion. The nature of the even (24) and the odd (25) sidebands is fundamentally different. Let θ be the angle between the probe beam, \hat{q} , and the direction the electric field is polarized in, \hat{z} , see Fig. 1. The even sidebands do not depend on θ . They can thus be regarded as a result of pure amplitude modulations of the fundamental probe. For the odd sidebands however, we note that $I_{2n+1} \propto \sin^2 \theta$. The odd sidebands therefore vanish when the probe is aligned parallel with the electric field, but is at a maximum when they are aligned perpendicular to each other.

Taking $d_{cv\uparrow\downarrow} = d_{cv\uparrow\uparrow}$ to be constant, we have evaluated the sideband intensities according to (24) and (25) using the material parameters for the heavy hole band and conduction band for GaAs and InAs. We have taken $\hbar\Omega = 30\text{meV}$ for the calculations. In Fig. 3 we show I_n , $n = 1, 2, 3, 4$, for THz intensities corresponding to $\gamma = 0.1, 0.5, 1.0, 2.0$ as a function of the probe frequency for GaAs. Near resonance I_2 is dominating. Moving away from the resonance I_1 decays much slower than the other sidebands and eventually becomes dominating. Notice also that $I_4 > I_3$ within the region shown. The even sidebands are more sensitive to the THz intensity than the odd sidebands. In Fig. 4 we show the results for InAs. Qualitatively the behavior is identical except that for the higher THz intensities we note that $I_4 < I_3 < I_2 < I_1$ away from resonance. Quantitatively the odd sidebands are about a factor 100 stronger than for GaAs. In Fig. 5 we show the same sideband intensities as a function of the THz intensity keeping the probe frequency fixed, $\omega/\Omega = 2.5, 5.0, 7.5, 10.0$, for GaAs. Note how I_2 and I_3 seem to rise in a similar manner. It is noteworthy as well how feature less I_1 is, in fact I_1 is mostly linear γ within the regimes we have investigated. In Fig. 6 we show the same results for InAs.

We have considered other possible sources of inversion symmetry breaking. Spin-orbit splitting due to the crystal field leads to a cubic contribution in the effective Hamiltonian for zinc-blend structures [23], which breaks the inversion symmetry. We find however that the contribution to the sidebands due to this term is three orders of magnitude less than the contribution due to (17) considered above for GaAs and InAs. Another possible source is the band bending at the edge of the sample due to the pinning of the Fermi level associated with charge accumulation of residual charge carriers at the surface of the sample. Thus the relevant inversion symmetry may be broken if the THz field has an electric field component perpendicular to the surface of the sample. We have assumed that this is not the case.

In summary, we have studied the nonlinear generation of optical sidebands in strongly THz driven undoped direct gap semiconductors. We have found that relativistic spin-THz field coupling leads to local breaking of inversion symmetry which results in the formation of, otherwise suppressed, odd sidebands in the transmitted wave of a weak near infrared interband probe. We have shown that the even sidebands are independent on the relative orientation of

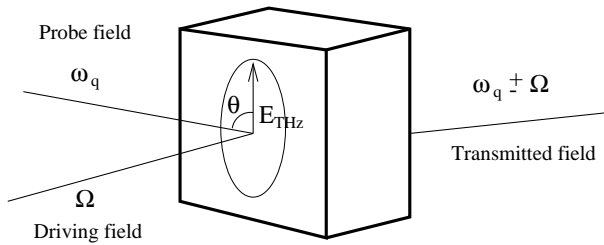


FIG. 1. Schematic illustration of the experimental setup, showing also the relative orientation of the probe and the linearly polarized THz electric field.

the probe and the linearly polarized THz field, while the odd sidebands depend strongly on the relative orientation of the probe to the THz field. The even sidebands dominate the transmission spectrum for probe frequencies near the gap, but moving the probe away from the gap odd sidebands will eventually dominate. We find that the relativistic effects are orders of magnitude stronger in InAs than in GaAs.

ACKNOWLEDGMENTS

We thank Dr. Antti-Pekka Jauho and Dr. Simon Pedersen for useful discussions on various inversion symmetry breaking effects in semiconductors, and in particular Dr. Junichiro Kono for discussing his experimental results prior to publication.

- [1] W. Franz, Z. Naturforschung **13**, 484 (1958); L. W. Keldysh, Sov. Phys. JETP **34**, 788 (1958).
- [2] Y. Yacoby, Phys. Rev. **169**, 610 (1968).
- [3] See, e.g., C. A. Brau, *Free-Electron Lasers* (Academic Press, San Diego, 1990).
- [4] K. Nordstrom *et al.*, phys. stat. sol. (b) **204**, 52 (1997).
- [5] J. Cerne *et al.*, Appl. Phys. Lett. **70**, 3543 (1997).
- [6] J. Kono *et al.*, Phys. Rev. Lett. **79**, 1758 (1997).
- [7] K. Nordstrom *et al.*, Phys. Rev. Lett. **81**, 457 (1998).
- [8] C. Phillips *et al.*, Appl. Phys. Lett. **75**, 2728 (1999).
- [9] T. Meier, F. Rossi, P. Thomas and S. W. Koch, Phys. Rev. Lett. **75**, 2558 (1995).
- [10] A.-P. Jauho and K. Johnsen, Phys. Rev. Lett. **76**, 4576 (1996).
- [11] L. Jonsson, M. M. Steiner, and J. W. Wilkins, Appl. Phys. Lett. **70**, 1140 (1997).
- [12] D. S. Citrin, Appl. Phys. Lett. **1189** (1997).
- [13] W. Xu, J. Phys.:Condens. Matter **10** 10787 (1998).
- [14] K. Johnsen and A.-P. Jauho, phys. stat. sol. (a) **164**, 553 (1997).
- [15] K. Johnsen and A.-P. Jauho, Phys. Rev. B **57**, 8860 (1998).
- [16] A. H. Chin, J. M. Bakker, and J. Kono, preprint (1999).
- [17] See, e.g., H. Haug and A.-P. Jauho, *Quantum Kinetics in Transport and Optics of Semiconductors*, Springer Series in Solid-State Sciences Vol. 123 (Springer, Berlin, 1996).
- [18] D. C. Langreth, NATO Advanced Study Institute Series B, **17**, edited by J. T. Devreese and E. van Doren (Plenum, New York, 1976).
- [19] See, e.g., J. J. Sakurai, *Advanced Quantum Mechanics*, (Reading, MA: Addison-Wesley, 1967).
- [20] B. Jusserand *et al.*, Phys. Rev. B, **51**, 4707 (1995).
- [21] W. Knap *et al.*, Phys. Rev. B, **53**, 3912 (1996).
- [22] Tue Hassenkam *et al.*, Phys. Rev. B, **55**, 9298 (1997).
- [23] G. Dreselhaus, Phys. Rev. **100**, 580 (1955).

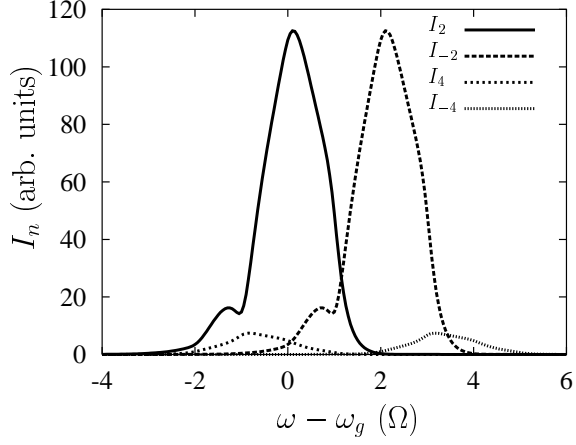


FIG. 2. Sideband intensities I_n as a function of the probe frequency using material parameters for GaAs, $\gamma = 1$ and $\hbar\Omega = 30\text{meV}$. Only even sidebands appear due to the inversion symmetry of the Hamiltonian. Note that $I_n(\omega) = I_{-n}(\omega + n\Omega)$.

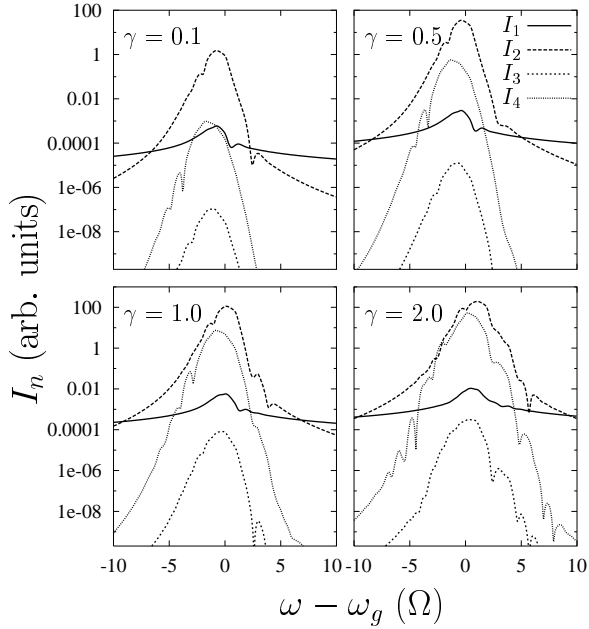


FIG. 3. Sideband intensities I_n , $n \in \{1, 2, 3, 4\}$, as a function of the probe frequency using material parameters for GaAs including the relativistic effects. Values of γ are 0.1, 0.5, 1.0 and 2.0 with $\hbar\Omega = 30\text{meV}$.

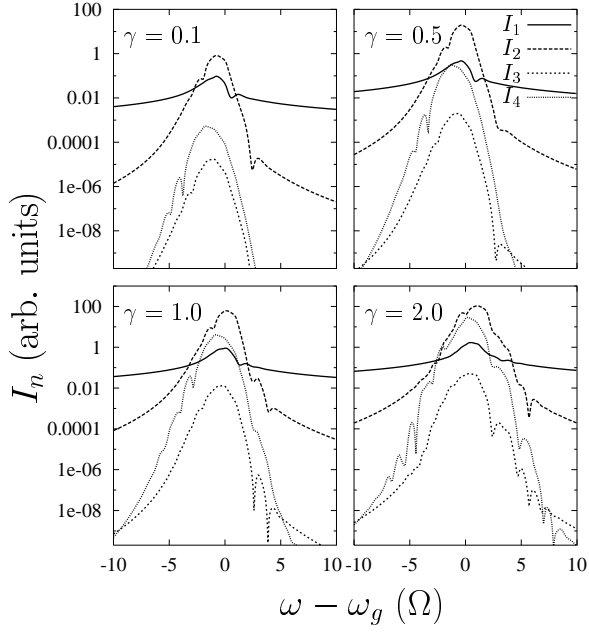


FIG. 4. Sideband intensities I_n , $n \in \{1, 2, 3, 4\}$, as a function of the probe frequency using material parameters for InAs including the relativistic effects. Values of γ are 0.1, 0.5, 1.0 and 2.0 with $\hbar\Omega = 30\text{meV}$.

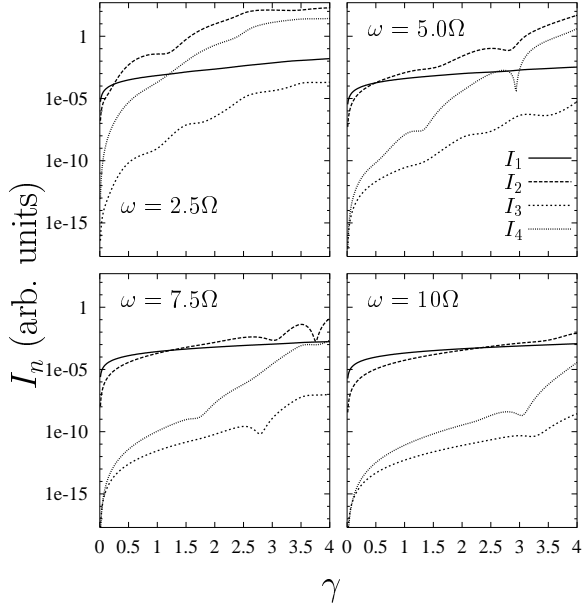


FIG. 5. Sideband intensities I_n , $n \in \{1, 2, 3, 4\}$, as a function of γ using material parameters for GaAs including the relativistic effects. Values of $\omega - \omega_g$ are 2.5Ω , 5.0Ω , 7.5Ω and 10.0Ω with $\hbar\Omega = 30\text{meV}$.

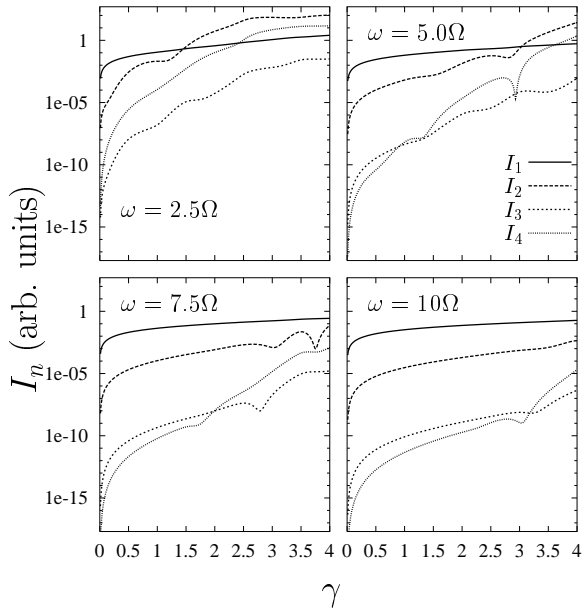


FIG. 6. Sideband intensities I_n , $n \in \{1, 2, 3, 4\}$, as a function of γ using material parameters for InAs including the relativistic effects. Values of $\omega - \omega_g$ are 2.5Ω , 5.0Ω , 7.5Ω and 10.0Ω with $\hbar\Omega = 30\text{meV}$.